26th ABCM International Congress of Mechanical Engineering
November 22-26, 2021. Florianópolis, SC, Brazil

VISCOELASTIC MODELING OF PORCINE LIGAMENTS

Bruno Mello Silveira
Stephanie Aguiar Salles de Barros
Departamento de Engenharia Mecânica - PPEMM - CEFET/RJ; Av. Maracanã, 229 – RJ – Brazil.
bruno.silveira@aluno.cefet-rj.br, stephanie.barros@aluno.cefet-rj.br

Rodrigo Ribeiro Pinho Rodarte
Programa de Pós-graduação em Engenharia Mecânica e Tecnologia de Materiais - PPEMM - CEFET/RJ; Av. Maracanã, 229 – RJ – Brazil. Instituto Nacional de Traumatologia e Ortopedia – INTO -Av. Brazil, 500, RJ, Brazil.
rodrigo.rodarte@aluno.cefet-rj.br

Paulo Pedro Kenedi
Programa de Pós-graduação em Engenharia Mecânica e Tecnologia de Materiais - PPEMM - CEFET/RJ; Av. Maracanã, 229 – RJ – Brazil. Departamento de Engenharia Mecânica – CEFET/RJ - Av. Maracanã, 229 – RJ – Brazil.
paulo.kenedi@cefet-rj.br

Abstract. *Viscoelastic quasi-linear analytical models, as Fung, was implemented through the utilization of experimental results obtained from several porcine ligaments as: lateral collateral ligament (LCL), anterior cruciate ligament (ACL), posterior cruciate ligament (PCL) and medial collateral ligament (MCL). To implement quasi-linear viscoelastic models for soft tissues, as the Fung one, it was necessary the utilization of a programming language, as C Sharp, and Object-oriented programming to deal with the model's mathematical demands, as the convolution calculations. Moreover, those technologies allow to reduce the code execution time, which was one of the main challenges. The numerical implementation of Fung's model successfully reproduces the stress evolution in relaxation tests.*

Keywords: *knee ligaments, analytic model, viscoelasticity, Fung*

1. INTRODUCTION

The knee is one of the most complex joints of the body and it is subjected to different loadings. The description of the mechanical behavior of the knee ligaments can be very useful to aid to model, quantitatively, the knee performance. Thus, researches have been published attempting to macroscopically analyze the knee ligaments/tendons through different viscoelastic mechanical models. (Rossetto, 2009) shows that this knowledge was important to better support the decisions relative to physical training, such as in cases of therapy for tendinopathies. (Bernardes et. al, 2005) sought to determine the biomechanical parameters for modeling the human knee joint through extensive exercises, together with images obtained by videofluoroscope, where the viscoelasticity was accessed.

Viscoelasticity is understood as the property of materials that present viscous and elastic behavior at the same time. This concept is widely used in various sectors of the industry. The simplest viscoelastic model is one that considers linear functions, where the creep compliance and stress relaxation functions are depending only on time. This approach is commonly used for metals. (Tareco, 2014) uses Maxwell and Kelvin linear models to design steel-concrete structures, analyzing the relaxation and creep compliance, just for the concrete, in the mixed structure response. Moreover, as presented by (Queiroz, 2008), viscoelastic materials are also used to attenuate vibrations and noise of structures, having application in both the automotive and aerospace sectors.

The quasi-linear viscoelastic model, proposed by (Fung, 1993), is commonly used to describe the soft tissues behavior. (Piazza et al., 2001) developed a three-dimensional dynamic model of a tibiofemoral and patellofemoral articulations, to predict the knee implant movements during a step-up activity. They were based on the Fung's model, using dynamic equations of motion subjected to forces generated by muscles, ligaments, and contact at articulations. Good results were achieved for the flexion-extension angle of the knee, but not for translations at the tibiofemoral articulations. (Debski et al, 2004) applied the Fung's model and analyzed the viscoelastic properties of the healing goat MCL. They characterized the reduced relaxation function and the elastic response, and demonstrated that que quasi-linear viscoelastic model could be successfully used to describe the MCL viscoelastic behavior, during the healing phase.

Moreover, the quasi-linear viscoelastic method is frequently employed with computational resources, since it has complex equations and not have any explicit analytical solution disponible. (Xu and Engquist, 2018) proposed a mathematical model for relaxation modulus based on nonlinear model and its numerical solution. They developed a finite-element framework and a numerical algorithm to implement this model for simulating responses under static and dynamic

loadings. They validated their model through the utilization of various materials, comparing experimental and numerical results. (Weiss et al, 2001) reviewed earlier and current techniques for the computational modeling of soft tissues, showing relevant concepts under the perspective of continuum mechanics and finite element method. Also, emphasized the microstructural influence of soft tissues. (Abramowitch et al., 2004) obtained the constants for quasi-linear viscoelastic model that are used to describe the elastic response, with constants A and B, and the reduced relaxation function, with constants C, τ_1 and τ_2, together with an improved approach that converges to a single solution with minimal variation. They subjected six goat femur-MCL-tibia to a uniaxial tensions test, considering the ramp time. In these tests, the convergence has failed for three ligaments, with the biggest errors at constants A, B e τ_1.

The aim of this paper is to explain the numerical implementation of the Fung's quasi-linear viscoelasticity model. Using the C# programming language, as in (Wagner et al, 2021) and ASP.NET MVC framework, as in (Rick Anderson, 2019) and (Gasparotto, 2014). (Silveira, 2020) developed a REST API capable of performing the necessary calculations for this model and generating a CSV file to compare the numerical results with the experimental ones. The API was developed focusing on scalability, maintainability, and readability, applying some design patterns, as Strategy, and object-oriented programming patterns, as SOLID principles. Some resources were, also, used to optimize the software, as Swagger, for building the user interface.

2. FUNG'S QUASI-LINEAR VISCOELASTIC MODEL

The quasi-linear viscoelastic model, (Fung, 1993), was proposed with a non-linearity stress-strain relation, divided in two parts: the reduced relaxation function, which depends only on time, and the elastic response, which depends on strain. This model is commonly used for soft tissue, with good performance. The constants needed for the equations must be obtained experimentally. However, the Fung's model has limitations, as for distinct relaxations and strain levels, different constants values must be found.

2.1 Mathematical description

(Fung, 1993) propose equations for elastic response, reduced relaxation function and stress considering one relaxation. For two relaxations, in sequence, considered in this paper, it was necessary to adapt these equations. Moreover, each parameter will be expressed accordingly when considering or disregarding ramp time, except for reduced relaxation function.

2.1.1 Strain application

The equations used to describe the strain were developed to represent the experiments. When considering ramp time, the strain behavior is expressed by equation (1). When the strain maintains at the maximum value ε_{max}, it represents the relaxation. When it stays at the minimum value ε_{min}, it represents the recovery. That behavior also is observed in (Duenwald, et al., 2009). When disregard ramp time, the equation (2) can be used, where is considered a constant strain during whole experiment.

$$\varepsilon(t) = \begin{cases} \lambda_1 \cdot t, & 0 \le t < t_0 \\ \varepsilon_{max}, & t_0 \le t < t_1 \\ \varepsilon_{max} - \lambda_2 \cdot (t - t_1), & t_1 \le t < t_2 \\ \varepsilon_{min}, & t_2 \le t < t_3 \\ \varepsilon_{min} + \lambda_1 \cdot (t - t_3), & t_3 \le t < t_4 \\ \varepsilon_{max}, & t \ge t_4 \end{cases}, \tag{1}$$

where, the parameters t_0 and λ represent, respectively, ramp time and strain rate applied in experiment, with λ_1 used when strain is increasing and λ_2, when it is decreasing. Furthermore, the parameters t_1, t_2, t_3 and t_4 are the time limits for each equation, indicating when the strain behavior changes.

$$\varepsilon(t) = \varepsilon_0, \tag{2}$$

where, ε_0 represents the constant strain applied through the experiment.

It is possible to calculate the derivative that will be used in the stress calculations step. The equations (3) and (4) are the time derivative of, respectively, equations (1) and (2).

$$\frac{d\varepsilon(t)}{dt} = \begin{cases} \lambda_1, & 0 \le t < t_0 \\ 0, & t_0 \le t < t_1 \\ -\lambda_2, & t_1 \le t < t_2 \\ 0, & t_2 \le t < t_3 \\ \lambda_1, & t_3 \le t < t_4 \\ 0, & t \ge t_4 \end{cases}, \tag{3}$$

$$\frac{d\varepsilon(t)}{dt} = 0. \tag{4}$$

Fig. 1 show the graphical representation of equations (1) and (3).

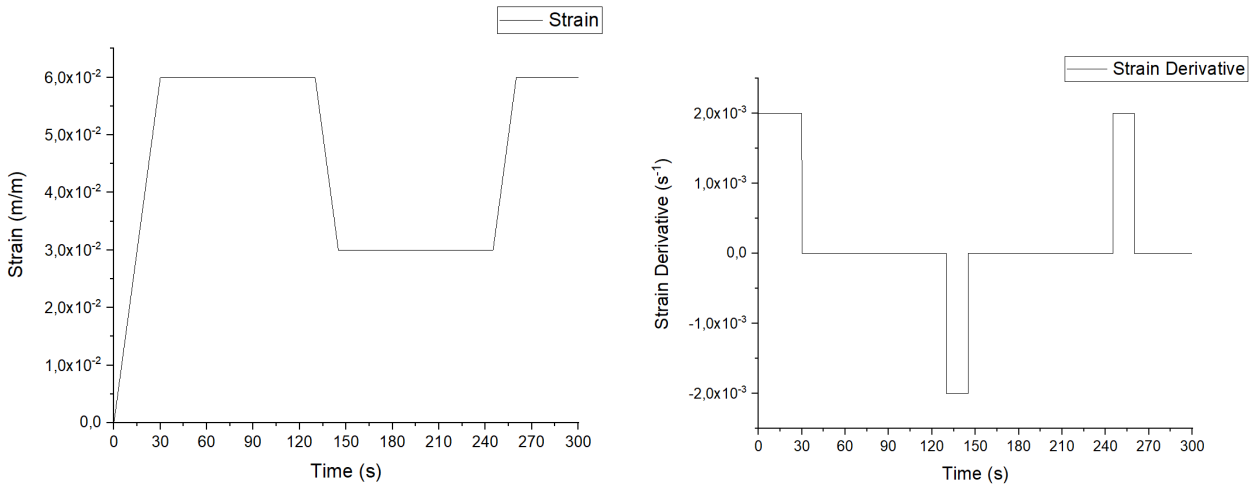

(a) (b)

Figure 1. (a) Strain vs time and (b) strain derivative vs time.

Note that, in Fig.1.a, the $\varepsilon_{min} = 3 \cdot 10^{-2}\ m/m$ and the $\varepsilon_{max} = 6 \cdot 10^{-2}\ m/m$. Also, the values of the strain derivatives in Fig.1.b depends on the ramp time. For instance, for the first ramp ($0 \le t < t_0$), the calculus was: $6 \cdot 10^{-2}/30 = 2 \cdot 10^{-3}\ s^{-1}$.

2.1.2 Stress response

The elastic and the viscoelastic stress responses are covered in this item.

Elastic response

The elastic response corresponds the soft tissue elastic part. As mentioned previously, two equations are used to describe the elastic response. When considering ramp time, an exponential approximation can be used like in research (Abramowitch, 2004).

$$\sigma_e(\varepsilon) = A \cdot (e^{B\varepsilon} - 1) \tag{5}$$

where constants *A*, in Pa (Pascal), and *B*, dimensionless, are material constants and represents, respectively, an elastic stress constant and an elastic power constant. Moreover, as shown previously, the equation (5) can be rewritten with only time dependence.

$$\sigma_e(t) = A \cdot \left(e^{B\varepsilon(t)} - 1\right) \tag{6}$$

The derivative for elastic response must be calculated because it will be used in equations for describing the stress evolution. The derivative, in time and in strain, of equation (5) are:

$$\frac{d\sigma_e(\varepsilon)}{d\varepsilon} = A \cdot B \cdot e^{B\varepsilon} \tag{7}$$

$$\frac{d\sigma_e(t)}{dt} = A \cdot B \cdot e^{B\varepsilon(t)} \cdot \frac{d\varepsilon(t)}{dt} \tag{8}$$

When disregarding ramp time, the elastic response is considered constant for all time domain.

$$\sigma_e(\varepsilon) = \sigma_e(t) = \sigma_0 \tag{9}$$

Where, σ_0 is the initial stress applied in the experiment. The derivative in time and in strain for equation (9) is:

$$\frac{d\sigma_e(\varepsilon)}{d\varepsilon} = \frac{d\sigma_e(t)}{dt} = 0 \tag{10}$$

Reduced relaxation function

The reduced relaxation function represents the viscous portion and occurs for all time domain and with **g**(0) = 1. (Fung, 1993) stated that it can be described in two ways: a) the equation (11), also called the simplified reduced relaxation function, is written using the Prony Series, taking only three elements in the sum, in line with (Babaei et al, 2015), that affirmed that three elements were sufficient for a good approximation. Also, (Funk et al., 2000) stated that more than three elements do not result in a significant gain. b) the equation (12), was developed from Kelvin model, standard linear solid, and uses integrals that only have numerical solutions. Moreover, both equations were implemented and tested in this research, but only the first one was effectively used, as their constants are easier to be calculated experimentally.

$$g(t) = \boldsymbol{G}_\infty + \sum_{i=1}^{3} \boldsymbol{G}_i \cdot e^{\frac{-t}{\tau_i}} \tag{11}$$

where $\boldsymbol{G}_\infty$ and $\boldsymbol{G}_i$ are material dimensionless constants called relaxation modulus and represents the amplitude of the stress curve in relaxation, and $\boldsymbol{\tau}_i$ is the relaxation time in seconds, also a material constant.

$$g(t) = \frac{1 + C \cdot \left[E_1\left(\frac{t}{\tau_2}\right) - E_1\left(\frac{t}{\tau_1}\right)\right]}{\left[1 + C \cdot \ln\left(\frac{\tau_2}{\tau_1}\right)\right]} \qquad where\ E_1(z) = \int_z^\infty \frac{e^{-x}}{x} dx \tag{12}$$

where C, τ_1 and τ_2 are material constants and represents, respectively, a dimensionless relaxation constant, fast and slow relaxation times in seconds. The equation (12) can be rewritten, with the development shown in Appendix:

$$g(t) = \frac{1 + C \cdot I(t)}{1 + C \cdot \ln\left(\frac{\tau_2}{\tau_1}\right)} \qquad where\ I(t) = \int_{\frac{t}{\tau_2}}^{\frac{t}{\tau_1}} \frac{e^{-x}}{x} dx \tag{13}$$

Also calculating the derivative in time of equation (13) for reduced relaxation function, in Appendix:

$$\frac{dg(t)}{dt} = \frac{C}{1 + C \cdot \ln\left(\frac{\tau_2}{\tau_1}\right)} \cdot \frac{e^{-\left(\frac{t}{\tau_1}\right)} - e^{-\left(\frac{t}{\tau_2}\right)}}{t} \tag{14}$$

(Fung, 1993) shows three equivalent equations to calculate the stress:

$$\boldsymbol{\sigma}(t) = \boldsymbol{\sigma_e}(0) \cdot \boldsymbol{g}(t) + \int_0^t \boldsymbol{g}(t-\tau) \frac{\partial \boldsymbol{\sigma_e}(\tau)}{\partial \tau} d\tau \tag{15}$$

$$\boldsymbol{\sigma}(t) = \boldsymbol{\sigma_e}(t) \cdot \boldsymbol{g}(0) + \int_0^t \boldsymbol{\sigma_e}(t-\tau) \cdot \frac{\partial \boldsymbol{g}(\tau)}{\partial \tau} d\tau \tag{16}$$

$$\boldsymbol{\sigma}(t) = \frac{\partial}{\partial t} \int_0^t \boldsymbol{\sigma_e}(t-\tau) \cdot \boldsymbol{g}(\tau) d\tau \tag{17}$$

As mentioned above, the elastic response and reduced relaxation function can be expressed only depending on time, so the partial derivative can be changed by total derivative. Moreover, $\boldsymbol{\sigma_e}(0) = 0$ and $\boldsymbol{g}(t) = 1$.

$$\boldsymbol{\sigma}(t) = \int_0^t \boldsymbol{g}(t-\tau) \cdot \frac{d\boldsymbol{\sigma_e}(\tau)}{d\tau} d\tau \tag{18}$$

$$\boldsymbol{\sigma}(t) = \boldsymbol{\sigma_e}(t) + \int_0^t \boldsymbol{\sigma_e}(t-\tau) \cdot \frac{d\boldsymbol{g}(\tau)}{d\tau} d\tau \tag{19}$$

$$\boldsymbol{\sigma}(t) = \frac{d}{dt} \int_0^t \boldsymbol{\sigma_e}(t-\tau) \cdot \boldsymbol{g}(\tau) d\tau \tag{20}$$

While considering ramp time, all equations return satisfactory results. Disregarding ramp time, the elastic response is constant, and its derivative is zero for all time domain, as shown previously. Thus, the equation (18) cannot be used, because it always returns zero, and equations (19) and (20) can be rewritten. As shown in Appendix, equations (19) and (20) return to the same equation (21). So, when disregarding ramp time, a unique equation can be used is:

$$\boldsymbol{\sigma}(t) = \boldsymbol{\sigma_e} \cdot \boldsymbol{g}(t) \tag{21}$$

Fig. 2.a show the graphical representation of equations (18-20) for the loading presented in Fig. 2.a and equivalently in Fig. 2.b for equation (21). For these graphs, where used the same constants for reduced relaxation function.

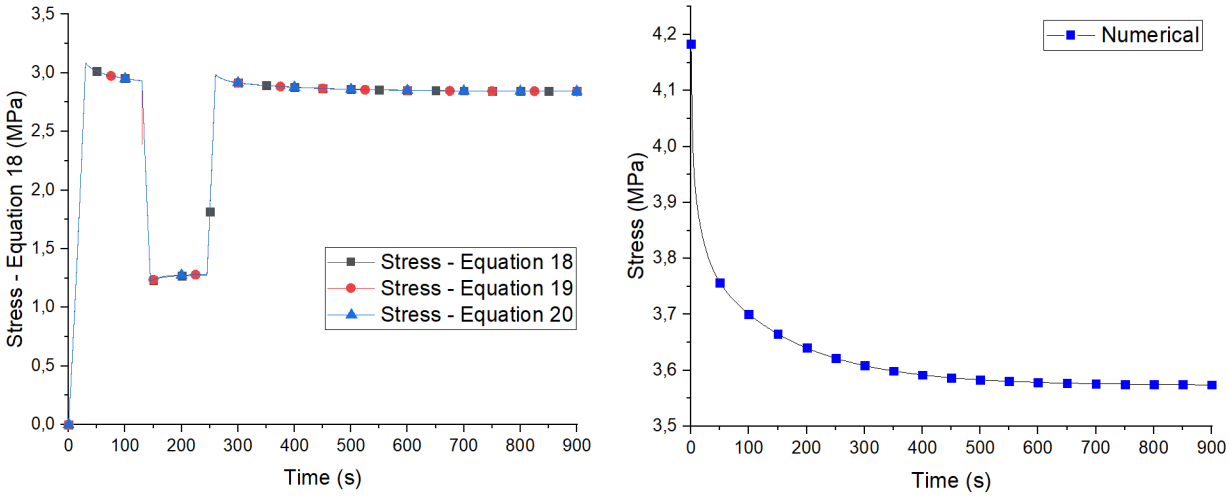

(a) (b)

Figure 2. Stress vs time using: (a) equations (18-20) and (b) equation (21).

In the next section the numerical implementation of the Fung's equations is fully explained.

3. NUMERICAL IMPLEMENTATION

The numerical implementation of Fung's Model was developed in two steps: creating a class that represents the model which contains the equations for each parameter and its respective derivative in time; and creating a class to orchestrate the operation. Also, it was created an artificial frontier in the code that separates the operation and the model, creating specific contracts for each one. It was done based on Single-Responsibility Principle that gets easier to implement resources, prevents unexpected side-effects and improves maintainability. It is noticeable that the execution time lasted for minutes and, in worst cases, for hours, because the equations used to calculate the stress were not optimized for numeric applications. To improve their performance, it was used the class Task, a native resource from C#, with the aim to allow some steps being processed asynchronously, executing multiple tasks together and reducing the execution time. It was used in both classes mentioned early, for calculating the results, and for iterating the input list, reducing that time to seconds, in worst case.

In Fig. 3 shows the flowchart for main operation that calculates the results for Fung's model and the respective sub-routine. The class that represents the model also contains a method, represented in Fig. 3 as sub-routine "Calculate

Results", that calculate, in parallel, all results necessaries - strain, elastic response, reduced relaxation function and stress – as shown in Fig. 3.b, returning those values in an object. The orchestrator is responsible to orchestrate the operation, executing each step shown on Fig. 3.a. Furthermore, the request data must be validated previously to avoid any error over code execution.

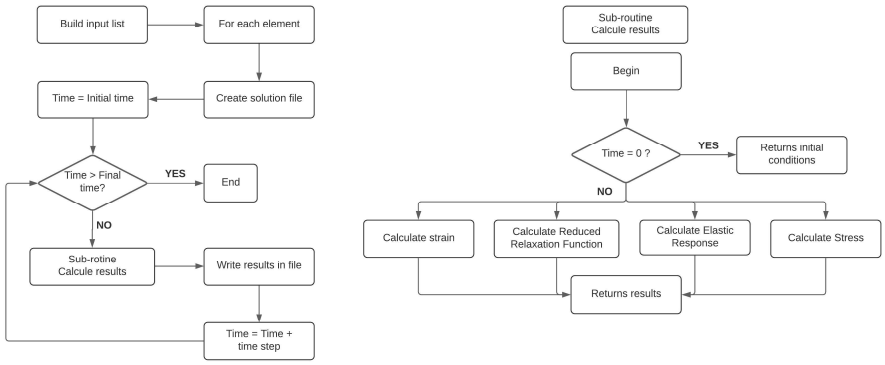

(a) (b)

Figure 3. Flowchart for (a) main operation and (b) sub-routine "Calculate Results".

It was, also necessary to implement numerical methods to deal with integrations and derivatives present in stress and reduced relaxation function equations. For the integrals, the Composite Simpson's Rule, stated in equation (22), available in (Regra de Simpson, 2021) (Regras Compostas, 2021), was used. For the derivatives, the Symmetric Derivative, stated in equation (23), available in (Da Cruz, 2012), was used.

$$\int_a^b f(x)dx = \frac{\Delta x}{3}\left[f(x_0) + 4\cdot\sum_{k=1}^{N/2} f(x_{2k-1}) + 2\cdot\sum_{k=1}^{(N/2)-1} f(x_{2k}) + f(x_N)\right] \tag{22}$$

where f(x) is an integrable function, *a* and *b* are the limits of integration, Δx is a differential of the variable *x*, and *N* is the number of subdivisions.

$$\frac{df(x)}{dx} = \frac{f(x+\Delta x) - f(x-\Delta x)}{2\Delta x} \tag{23}$$

where f(x) is a differentiable function and Δx is a differential of the variable x.

Numerical extrapolation

Besides the numerical implementation of the quasi-linear viscoelastic model, for a better comparison with experimental results, it was necessary to develop a routine for extrapolating the experimental results. For implement this, it was necessary to predict the next values based on the earlier stress curves' behavior. Considering that during relaxation there are two important behaviors occurring: the stress decreases on time and the concavity has upwards direction. These typical behaviors were used to validate each point before applying extrapolation, to remove invalid points that could interfere in the final extrapolated results.

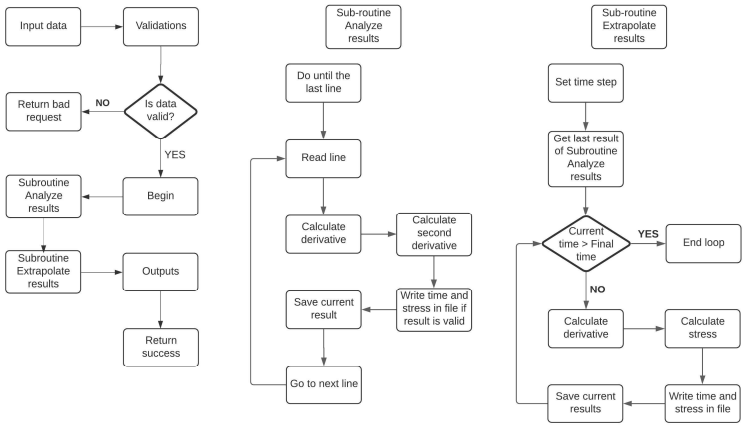

Figure 4. Flowchart for numerical extrapolation.

The numerical extrapolation was made according to Fig. 4 flowchart. It worth mentioning that after the API receives input data, these are validated to ensure that the file has enough lines for the operation and the parameters that were passed were correct. The operation was divided in two subroutines to improve maintainability and readability, since the software may be used in future research.

4. RESULTS AND CONCLUSIONS

The numerical results obtained coincide with the experimental ones. In Fig. 5 shows the comparison between these values when disregarding the ramp time, which is the consideration proposed in the Fung's model, where assumes that the initial stress is applied as fast as a step. These graphs are equivalent to the ones shown in Fig.2.b.

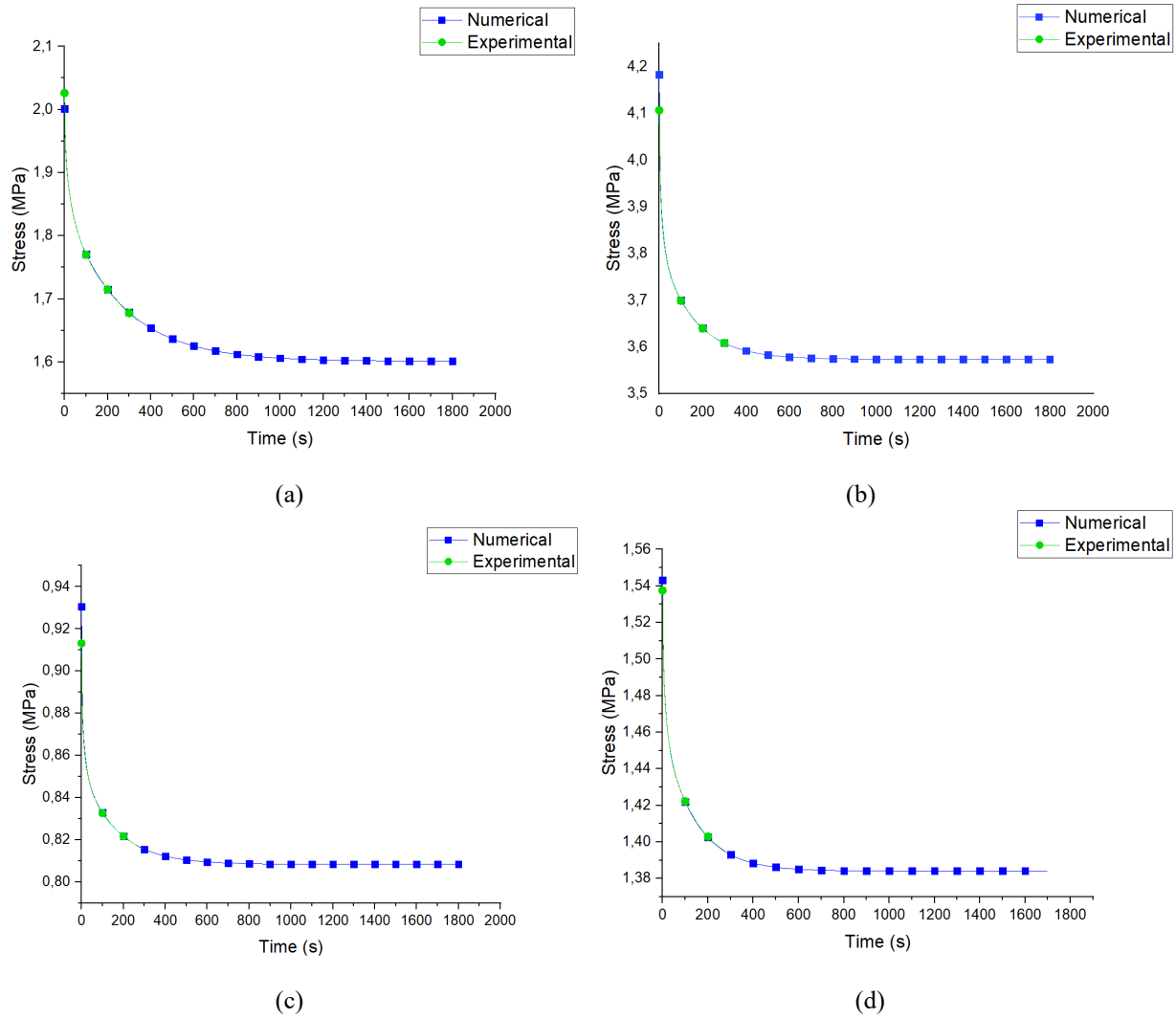

Figure 5. Stress vs time for (a) ACL, (b) LCL, (c) MCL and LCP. (The the experimental results were obtained by the same CEFET/RJ's research group)

As shown in Fig. 5, it was possible to reproduce the experimental behavior using the Fung's model equations. The first part of these graphics the experimental and the numerical points are directly compared (up to about 300 s). Thenceforth the points are just numerical, from extrapolation calculations.

The numerical implementation of the Fung's model was quite successful. All step, both mathematical and software implementation, were fully covered by this text. Beyond the reliable reproduction of experimental results, the extrapolation of the relaxation experimental data, up to an asymptotic behavior, proved to be consistent.

This text covers the numerical part of an extensive research about the porcine ligaments mechanical characterization, with focus in their viscoelastic behavior. The earliest experimental results of this research have already been collected and they were used in this text as reference.

With the development of this research, the porcine ligaments experimental/numerical results can be utilized, as a first step, to increase the knowledge about the mechanical performance of human knees.

5. ACKNOWLEDGEMENTS

Bruno Mello Silveira and Stephanie Aguiar Salles de Barros are grateful for scholarship granted by CNPq.

6. REFERENCES

Abramowitch, Steven D. e Woo, Savio L.-Y., 2004. “An Improved Method to Analyze the Stress Relaxation of Ligaments Following a Finite Ramp Time Based on the Quasi-Linear Viscoelastic Theory”. *Journal of Biomechanical Engineering*. ASME. Vol. 126. P. 92-97. DOI: 10.1115/1.1645528.

Babaei, Behzad, et al. 2015. “Efficient and optimized identification of generalized Maxwell viscoelastic relaxation spectra”. *Journal of the Mechanical Behavior of Biomedical Materials*. Vol. 55, pp. 32-41. Available in: http://dx.doi.org/10.1016/j.jmbbm.2015.10.008. Accessed on May 6, 2021.

Bernardes, C., et al. 2005. “Biomechanical parameters' determination for knee joint modeling”. Laboratório de Pesquisa do Exercício, Universidade Federal do Rio Grande do Sul. Porto Alegre.

Da Cruz, A. M.C. B., Martins, N., Torres, D. F.M. 2012. “Symmetric differentiation on time scales”. *Applied Mathematics Letters*, Vol. 60, No. 2, pp.264-269. DOI:10.1016/j.aml.2012.09.005.

De Pascalis, R.; Abrahams, I.D.; Parnell, W.J.. 2014. “On nonlinear viscoelastic deformations: a reappraisal of Fung’s quasi-linear viscoelastic model”. *Proceedings of the Royal Society A: Mathematical, Physical and Engineering Sciences*. DOI: 10.1098/rspa.2014.0058.

Debski, R. E; Abramowitch, S. D.; Woo, S. L.-Y.; Clineff, T. D. 2004. “An evaluation of the quasi-linear viscoelastic properties of the healing medial collateral ligament in a goat model”. *Annals of Biomedical Engineering*. DOI: 10.1023/b:abme.0000017539.85245.6a.

Duenwald, S. E.; Jr., R. V.; Lakes, R. S., 2009. “Viscoelastic Relaxation and Recovery of Tendon”. University of Wisconsin-Madison. Madison, USA.

Fung, Y. 1993. “Biomechanics: Mechanical Properties of Living Tissues”. Springer, New York, University of Michigan.

Funk, J. R., Hall, G. W., Crandall, J. R., Pilkey, W. D., 2000. “Linear and quasi-linear viscoelastic characterization of ankle ligaments”. Journal of Biomechanical Engineering, Vol. 122, No. 1, p. 15-22. DOI:10.1115/1.429623.

Gasparotto, H. M. 2014. “ASP.NET MVC Introduction”. DEVMEDIA. 2014. Available in: devmedia.com.br/introducao-ao-asp-net-mvc/31878. Accessed on June 19, 2021.

Piazza, Stephen J.; Delp, Scott L. 2001. “Three-Dimensional Dynamic Simulation of Total Knee Replacement Motion During a Step-Up Task”. *Journal of Biomechanical Engineering*. ASME. Vol. 123. P. 599-606. DOI: 10.1115/1.1406950.

Queiroz, José Aparecido Silva de. 2008. “Flexible structures analysis with viscoelastic materials application”. Universidade Estadual Paulista, Faculdade de Engenharia de Bauru, 2008. Available in: https://repositorioslatinoamericanos.uchile.cl/handle/2250/2568006. Accessed on May 4, 2021.

Regra de Simpson. Instituto Superior Técnico de Lisboa. Available in: https://www.math.tecnico.ulisboa.pt/.Accessed on: May 18, 2021.

Regras Compostas. Universidade Federal do Rio Grande do Sul. Available in: https://www.ufrgs.br/reamat/ CalculoNumerico/livro-oct/in-regras_compostas.html. Accessed on May 18, 2021.

Rick Anderson. 2019. “ASP.NET overview”. Microsoft. Available in: https://docs.microsoft.com/en-us/aspnet/overview. Accessed on June 19, 2021.

Rossetto, N. P. 2009. “Viscosity in stretching tendons”. Universidade Estadual de Campinas. Campinas.

Silveira, B. M. 2020. “SoftTissue”. Available in: https://github.com/M3110/SoftTissue. Accessed on June 01, 2021.

Tareco, M. A. C. 2014. Conceitos de viscoelasticidade na modelação da fluência em estruturas mistas aço-betão. 154f. Dissertação (Mestrado) – Engenharia Civil, Faculdade de Ciências e Tecnologia. Lisboa, 2014. Available in: https://run.unl.pt/bitstream/10362/12481/1/Tareco_2014.pdf. Accessed on May 4, 2021.

Wagner, B., et al. 2021. “A tour of the C# language”. Microsoft. Available in: https://docs.microsoft.com/en-us/dotnet/csharp/tour-of-csharp/. Accessed on: June 14, 2021.

Weiss, Jeffrey A. e Gardiner, John C. 2001. “Computational Modeling of Ligament Mechanics”. University of Utah, Department of Bioengineering, Salt Lake City, Utah 84112.

Xu, Qinwu e Engquist, Björn. 2018. “A mathematical model for fitting and predicting relaxation modulus and simulating viscoelastic responses”. *Proceedings of the Royal Society A: Mathematical, Physical and Engineering Sciences*. DOI: 10.6084/m9.figshare.c.4088969.

Zheng, N.; et al. 1998. “An analytical model of knee for estimation of internal forces during exercise”. American Sports Medicine Institute. Birmingham, Alabama, USA.

7. APPENDIX

7.1 Development from equation (12) to equation (13)

Based on material properties and the constants definition, it can be assumed that $\tau_2 > \tau_1$, so, $\frac{t}{\tau_2} < \frac{t}{\tau_1}$, therefore, $E_1\left(\frac{t}{\tau_2}\right)$ could be rewritten like:

$$E_1\left(\frac{t}{\tau_2}\right) = \int_{\frac{t}{\tau_2}}^{\infty} \frac{e^{-x}}{x} dx = \int_{\frac{t}{\tau_2}}^{\frac{t}{\tau_1}} \frac{e^{-x}}{x} dx + \int_{\frac{t}{\tau_1}}^{\infty} \frac{e^{-x}}{x} dx, \tag{i}$$

Then:

$$E_1\left(\frac{t}{\tau_2}\right) - E_1\left(\frac{t}{\tau_1}\right) = \int_{\frac{t}{\tau_2}}^{\frac{t}{\tau_1}} \frac{e^{-x}}{x} dx + \int_{\frac{t}{\tau_1}}^{\infty} \frac{e^{-x}}{x} dx - \int_{\frac{t}{\tau_1}}^{\infty} \frac{e^{-x}}{x} dx = \int_{\frac{t}{\tau_2}}^{\frac{t}{\tau_1}} \frac{e^{-x}}{x} dx, \tag{ii}$$

Applying equation (ii) in (12):

$$g(t) = \frac{1+C\cdot I(t)}{1+C\cdot\ln\left(\frac{\tau_2}{\tau_1}\right)}, \qquad with\ I(t) = \int_{\frac{t}{\tau_2}}^{\frac{t}{\tau_1}} \frac{e^{-x}}{x} dx, \tag{13}$$

7.2 Development from equation (13) to equation (14)

Deriving (13) in function of time:

$$\frac{dg(t)}{dt} = \frac{d}{dt}\left[\frac{1+C\cdot I(t)}{1+C\cdot\ln\left(\frac{\tau_2}{\tau_1}\right)}\right] = \frac{C}{1+C\cdot\ln\left(\frac{\tau_2}{\tau_1}\right)} \cdot \frac{d}{dt}[I(t)],\ \ where\ \frac{d}{dt}[I(t)] = \frac{d}{dt}\left[\int_{\frac{t}{\tau_2}}^{\frac{t}{\tau_1}} \frac{e^{-x}}{x} dx\right], \tag{iii}$$

Applying the definition of calculus to the derivative of a definite integral:

$$\frac{d}{dt}\int_b^a f(x)dx = \frac{d}{dt}[F(a) - F(b)] = f(a)\cdot\frac{da}{dt} - f(b)\cdot\frac{db}{dt}, \tag{iv}$$

where $f(x) = \frac{e^{-x}}{x}$, $a = \frac{t}{\tau_1}$ and $b = \frac{t}{\tau_2}$.

$$\frac{d}{dt}\left[\int_{\frac{t}{\tau_2}}^{\frac{t}{\tau_1}} \frac{e^{-x}}{x} dx\right] = \frac{e^{-\frac{t}{\tau_1}}}{\frac{t}{\tau_1}} \cdot \frac{d}{dt}\left(\frac{t}{\tau_1}\right) - \frac{e^{-\frac{t}{\tau_2}}}{\frac{t}{\tau_2}} \cdot \frac{d}{dt}\left(\frac{t}{\tau_2}\right) = \frac{e^{-\frac{t}{\tau_1}}}{\frac{t}{\tau_1}} \cdot \frac{1}{\tau_1} - \frac{e^{-\frac{t}{\tau_2}}}{\frac{t}{\tau_2}} \cdot \frac{1}{\tau_2} = \frac{e^{-\frac{t}{\tau_1}} - e^{-\frac{t}{\tau_2}}}{t}, \tag{v}$$

Applying (v) in (iii):

$$\frac{dg(t)}{dt} = \frac{C}{1+C\cdot\ln\left(\frac{\tau_2}{\tau_1}\right)} \cdot \frac{e^{-\frac{t}{\tau_1}} - e^{-\frac{t}{\tau_2}}}{t}, \tag{14}$$

7.3 Development from equation (19) and (20) to equation (21)

Rewriting (19):

$$\boldsymbol{\sigma}(t) = \boldsymbol{\sigma_e} + \int_0^t \boldsymbol{\sigma_e} \cdot \frac{d\boldsymbol{g}(\tau)}{d\tau} d\tau = \boldsymbol{\sigma_e} + \boldsymbol{\sigma_e} \cdot \int_0^t \frac{d\boldsymbol{g}(\tau)}{d\tau} d\tau,$$

$$\boldsymbol{\sigma}(t) = \boldsymbol{\sigma_e} + \boldsymbol{\sigma_e} \cdot \big(\boldsymbol{g}(t) - \boldsymbol{g}(0)\big) = \boldsymbol{\sigma_e} + \boldsymbol{\sigma_e} \cdot (\boldsymbol{g}(t) - 1),$$

$$\boldsymbol{\sigma}(t) = \boldsymbol{\sigma_e} \cdot \boldsymbol{g}(t). \tag{21}$$

Rewriting (20):

$$\boldsymbol{\sigma}(t) = \frac{d}{dt}\int_0^t \boldsymbol{\sigma_e} \cdot \boldsymbol{g}(\tau) d\tau = \boldsymbol{\sigma_e} \cdot \frac{d}{dt}\int_0^t \boldsymbol{g}(\tau) d\tau,$$

$$\boldsymbol{\sigma}(t) = \boldsymbol{\sigma_e} \cdot \boldsymbol{g}(t). \qquad \text{(repeated)} \qquad (21)$$

8. RESPONSIBILITY NOTICE

The authors are the only responsible for the printed material included in this paper.